Longitudinal effective mass and band structure of quasiperiodic Fibonacci superlattices

A. Bruno-Alfonso,* F. J. Ribeiro, and A. Latgé
Instituto de Física, Universidade Federal Fluminense (UFF), Avenida Litorânea sn, 24210-340, Niterói, Rio de Janeiro, Brazil

L. E. Oliveira
Instituto de Física, Universidade Estadual de Campinas (UNICAMP), Caixa Postal 6165, 13083-970, Campinas, São Paulo, Brazil
(Received 26 June 1998; revised manuscript received 24 August 1998)

A systematic study of the longitudinal effective mass associated with either shallow impurity states or conduction Landau levels under in-plane magnetic fields is presented for Fibonacci superlattices. We analyze the relation between the mean longitudinal effective masses and the localization length of the corresponding electronic or impurity states. Under appropriate conditions we show that the mean longitudinal effective mass weakly depends on the nature of the electron state and localization length, and is essentially related to the Cantor-like energy spectra or ''band structure.'' [S0163-1829(99)02003-2]

I. INTRODUCTION

Quasicrystals have been intensively studied after their discovery by Shechtman *et al.*[1] in 1984, with special interest in the electronic properties[2–6] of these ordered but nonperiodic materials. Indeed, the ideal quasicrystal lattices follow quasiperiodic laws.[7] For electrons, one-dimensional quasiperiodic systems have Cantor-set-like energy spectra with self-similar and critical wave functions.[8–10] In semiconductor physics great interest on quasiperiodic systems emerged after 1985, when the first Ga-As-AlAs Fibonacci superlattice (FSL) was grown and characterized.[11] The study of conduction and valence electron states in GaAs-(Ga,Al)As FSL's were reported by Laruelle and Etienne,[12] with a detailed analysis of self-similar spectra and localization of wave functions together with the identification of peaks in photoluminescence excitation (PLE) spectra. Yamaguchi *et al.*[13] investigated the electronic structure and the perpendicular-transport properties of photoexcited carriers in a GaAs-AlAs Fibonacci superlattice by means of PLE spectroscopy and picosecond luminescence measurements. Normal-incidence reflectance spectra of GaAs-(Ga,Al)As FSL were obtained and characterized by Munzar *et al.*[14] based on calculations of the fractal-electronic spectrum. The electroabsorption and photorefractive properties of long-period GaAs-(Ga,Al)As FSL's were studied by Dinu, Melloch, and Nolte[15] to assess their potential use in broad-band diffraction devices. A detailed study of the dynamics of electronic-wave packets in semiconductor FSL's was presented by Diez *et al.*,[16] where the authors show that propagation is determined by the fractal-like electron-energy spectrum. Theoretically, the localization properties of electron wave functions of FSL's have received special attention,[17,18] and the effects of electric fields have been calculated and analyzed.[19–22] However, little attention has been dedicated to a possible extension of the useful effective-mass concept to quasiperiodic solids. In this respect, only few calculations of the effective mass for Fibonacci superlattices have been reported,[23–25] and a direct relation of the effective mass with the energy-spectrum properties of these systems has not been remarked.

In the study of crystals the effective mass plays a central role since it contains relevant information about the band structure of such periodic systems, for which the Bloch theorem applies.[26] The energy-band structure is the base for theoretical studies of electronic properties of the solid, and the periodicity of the system is an essential condition for the existence of such bands together with the corresponding Brillouin zones. For semiconductor crystals in particular, the effective mass for the band edges of the fundamental gap describes most of the physics of carriers in both conduction and valence bands. A longitudinal effective mass (LEM) associated to the first-energy miniband (for conduction electrons, for instance) may be defined for periodic superlattices. The LEM value is apparent in electronic properties of these structures under certain conditions such as small period and weak barriers. However, for an ideal quasiperiodic system the Cantor-set nature of the electronic spectrum excludes the existence of bands. Hence the LEM concept, if meaningful, should not be introduced in the same usual way as for periodic systems. Shung, Sander, and Merlin,[23,24] following a one-dimensional approach, proposed a LEM associated to impurity states in FSL's. They also stated that this mass is possibly the relevant object for the cyclotron resonance and wave-packet propagation in quasicrystals. The calculated LEM is a quasiperiodic function of the impurity position, and when averaged over the whole system becomes almost independent of the system size for long Fibonacci sequences, converging to a value that increases with the impurity size.[23] A detailed study of shallow-donor impurity states in semiconductor FSL's was recently reported by Bruno-Alfonso, de Dios-Leyva, and Oliveira[25] within the effective mass and parabolic band approximations. They present a full discussion of the effects of the quasiperiodic and self-similar properties of the system on the 1*s*-like impurity states following different variational approaches. The superlattices considered are periodic stackings of a unit cell generated following a given Fibonacci sequence, and reach the quasiperiodic features for sufficiently large unit cells. A study of the LEM was performed,[25] by fixing the in-plane effective mass as the GaAs bulk value, and determining a LEM for each impurity

position and corresponding binding-energy value. In the present paper we report a discussion on the physical interpretations of the LEM associated with shallow-impurity states, together with a similar study of a LEM defined for Landau levels in the presence of in-plane magnetic fields (without impurities). The conditions for the LEM values to be associated with parabolic envelope curves of the FSL ''band structure'' within a wide range of localization radii of impurity or Landau states are discussed. The 1*s*-like impurity density of states is calculated and it is shown to become independent of the Fibonacci-sequence size as this size grows, as predicted before.[25]

II. THEORETICAL FRAMEWORK

We deal with shallow-donor impurity states and conduction Landau states (for in-plane magnetic fields) in Fibonacci superlattices that are actually periodic stackings of Fibonacci sequences of semiconductor layers (cyclic boundary conditions). The unit cell for the FSL of order n is the sequence ω_n of the elements a (a layer of $Ga_{1-x}Al_xAs$ of thickness d_a) and b (a layer of GaAs of thickness d_b), being $\omega_1=a$, $\omega_2=b$, and $\omega_n=\omega_{n-1}\omega_{n-2}$. The electron states are treated within the effective mass and parabolic-band approximations, with a constant effective-mass value (taken as 0.067 m_0) along the FSL.

The Hamiltonian of a single hydrogenic impurity in a GaAs-(Ga,Al)As superlattice (SL) with symmetry axis along the z direction may be written as

$$\hat{H}=\frac{\hat{\mathbf{p}}^2}{2m^*}-\frac{e^2}{\epsilon_r\sqrt{x^2+y^2+(z-z_i)^2}}+V_{SL}(z), \tag{1}$$

where m^* and ϵ_r are the effective mass and the static-dielectric constant of GaAs, respectively, and z_i is the impurity position. The SL potential $V_{SL}(z)$ is defined by the sequence of wells and barriers, corresponding to GaAs and (Ga,Al)As layers, respectively. The trial carrier-envelope wave function for the 1*s*-like state is chosen to be[25]

$$\Psi_a(x,y,z)=N\exp\left(-\frac{1}{a}\sqrt{x^2+y^2}\right)\psi_a(z), \tag{2}$$

where N is a normalization factor, a is a parameter that was previously chosen[25] to satisfy the bulk binding-energy limit, and $\psi_a(z)$ is to be determined via a variational scheme that minimizes the energy of the impurity ground-state given by Eq. (1). This procedure reduces the problem to a one-dimensional Schrödinger equation for $\psi_a(z)$ with the Hamiltonian given by

$$\hat{H}_{1D}=-\frac{\hbar^2}{2m^*}\frac{d^2}{dz^2}+U_a(z-z_i)+V_{SL}(z), \tag{3}$$

where

$$U_a(z)=R_y^*\left[\left(\frac{a^*}{a}\right)^2-\frac{4a^*}{a}G\left(\frac{z}{a}\right)\right], \tag{4}$$

with R_y^* and a^* being the GaAs effective Rydberg and Bohr radius, respectively, and

$$G(x)=\int_0^\infty\frac{2te^{-2t}}{\sqrt{t^2+x^2}}dt. \tag{5}$$

Notice that the second term in the 1D Hamiltonian corresponds to an effective one-dimensional potential for the electron-impurity interaction. Here, in contrast to the model by Shung *et al.*,[23] the confining potential parameters are determined by the bulk-effective mass and dielectric constant, except for the variational parameter a, which is determined by minimizing the lowest eigenenergy of H_{1D}, for each impurity position. It should be noted that the later minimization scheme is needed for thick-barrier superlattices as pointed out by Ribeiro, Bruno-Alfonso, and Latgé.[27]

For the case of conduction-electron Landau states in FSL's under in-plane magnetic fields a one-dimensional Schrödinger equation is also obtained for the carrier dynamics in the system-growth direction, by using an appropriate gauge for the field.[28–30] Here we solve the differential equation by trigonometric Fourier expansion and diagonalization techniques,[31] and take only the ground Landau level for each cyclotron-resonance center. For each center we determine a LEM (the in-plane effective mass is taken as the GaAs bulk value), which accounts for the ΔE energy difference between the actual Landau ground state and the ground level in the absence of magnetic field. For an effective anisotropic medium with in-plane effective mass m_ρ it is then easy to show that the LEM for an in-plane magnetic field B is

$$\frac{1}{m_\rho}\left(\frac{\hbar eB}{2\Delta E}\right)^2. \tag{6}$$

Of course, as in the case of the LEM associated with impurity states, the existence of a mean effective mass for the structure would be of great interest. This mass may be obtained, for instance, from an analysis of the absorption or photoluminescence spectra that present structures associated to van Hove–like singularities of the combined density of states. The intraband absorption coefficient of GaAs-(Ga,Al)As FSL's reported by de Dios-Leyva *et al.*[32] essentially illustrates this situation, and the same applies for transitions between donor and the conduction or valence states, from which it would be possible to determine a mean LEM value. However, in the present paper we adopt a simple approach in which the mean LEM value for the FSL may be associated either to the mean impurity binding energy or to the mean ΔE energy value, in the case of conduction Landau levels. In what follows we show that the mean LEM may be closely related to the SL ''band structure'' for different Fibonacci sequences.

III. RESULTS AND DISCUSSION

We first show in Fig. 1(a) the calculated donor shallow-impurity binding energy as a function of the impurity position in a GaAs-$Ga_{0.8}Al_{0.2}As$ FSL with 144 elements (order 12). The barrier and well thicknesses are 11.2 and 16.9 Å, respectively, and the dielectric constant is chosen as 12.5. The quasiperiodiclike behavior is apparent in this curve, which can be seen as a Fibonacci sequence of well-defined repeated patterns.[25] The shallow-donor density of states[33] (DOS) is displayed in Fig. 1(b) for the homogeneously *n*-

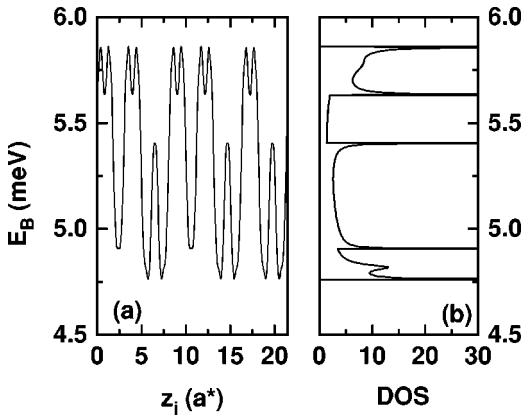

FIG. 1. (a) Donor shallow-impurity binding energy E_B as a function of the impurity position z_i (in units of the GaAs effective radius a^*), and (b) the associated shallow-impurity density of states (DOS), in a GaAs-$Ga_{0.8}Al_{0.2}As$ FSL with 144 elements (order 12). The barrier and well thicknesses are 11.2 and 16.9 Å, respectively, and the dielectric constant is 12.5. In (b) the FSL is supposed to be homogeneously *n*-type doped.

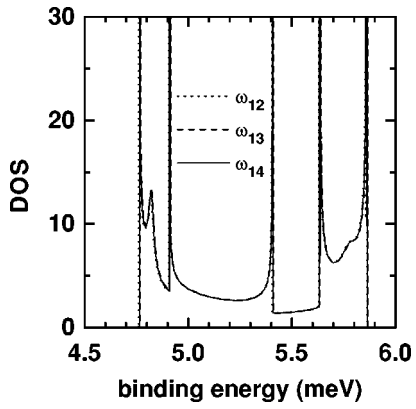

FIG. 2. As in Fig. 1(b), but for the Fibonacci sequences ω_{12}, ω_{13}, and ω_{14}, with 144, 233, and 377 elements, respectively.

type doped FSL. Some of the van Hove–like singularities in Fig. 1(b) may be associated with centers of local symmetry for the FSL. One should notice that centers of local symmetry occur with different radii in FSL's consisting of Fibonacci sequences of homogeneous semiconductor layers. The FSL built-in potential has this property, and the centers of symmetry in a one-dimensional approach would correspond to planes in a three-dimensional picture. A particle at such a plane of local symmetry will ''feel'' the same potential in both directions away from a plane of symmetry, up to a distance of the order of the corresponding symmetry radius. Of course, the centers of local symmetry are closely related to the hierarchy and self-similarity of the Fibonacci sequences. An essential condition for local symmetry centers to exist in FSL's is the symmetry of the elemental building blocks (*a* and *b*), which is satisfied in our case of homogeneous semiconductor layers. Also, one has symmetric subsequences in a given Fibonacci cell such as *bb, bab, aba, abba, abbabba*, and so on. One then finds that following the hierarchical quasiperiodic structure of the Fibonacci sequences, different symmetric subsequences with size near those of low-order Fibonacci blocks appear in a given FSL, and that equivalent subsequences are distributed following Fibonacci lattices. The van Hove–like singularities [cf. Fig. 1(b)] correspond to stationary points in the dependence of the impurity binding energy on the impurity position along the FSL growth direction [Fig. 1(a)]. For 1*s*-like impurity states only centers of local symmetry with radius larger than the impurity size (i.e., localization radius of the bound carrier, which can be estimated as 3 times the effective Bohr radius) will be apparent as local symmetry centers of the binding-energy curves. Of course, these centers of symmetry are stationary points, and hence correspond to van Hove–like singularities. However, other stationary points with their corresponding van Hove–like singularities exist, which are not symmetry centers for the impurity states with the same localization radius, as it is the case of the upper and lower edges of the ''impurity band'' in Fig. 1(a).

Figure 2 shows the shallow-donor DOS for ω_{12} as in Fig. 1(b), and also includes the DOS for the Fibonacci sequences ω_{13} and ω_{14}, with 233 and 377 elements, respectively. It may be seen that all curves essentially coincide, reflecting the independence of the DOS on the size of the FSL unit cell for sufficiently large Fibonacci-sequence orders. This is a clear consequence of the quasiperiodic behavior of the impurity bands, as discussed in detail by Bruno-Alfonso, de Dios-Leyva, and Oliveira.[25] Moreover, for the impurity states, if one considers the cyclic boundary conditions, it may be demonstrated that if one has the impurity band for a FSL of a given order expressed as Fibonacci sequence of two pieces, then all FSL's with larger order will have impurity bands that may be seen as Fibonacci sequences of the same pieces of curve. The system DOS can be expressed as the sum of the DOS of each one of the two pieces times their frequency in the Fibonacci cell, which are consecutive Fibonacci numbers. Since the ratio of consecutive Fibonacci numbers rapidly converges to the golden mean value, the normalized density of states becomes independent of the size of the FSL for sufficiently large systems. This property of the DOS is associated to the convergence of both the mean-impurity binding energy and related standard deviation as the size of the Fibonacci sequence increases, as discussed below.

Figure 3(a) shows the mean-impurity binding energy as a function of the order of the Fibonacci sequence that generates the unit cell. The FSL parameters are the same as above in one case ($\epsilon_r = 12.5$, which stands for the GaAs dielectric constant). Based on the assumption that it is the confining Coulomb potential that essentially determines the localization radius of the carrier,[29] the dielectric constant is the appropriated variable to theoretically study the LEM dependence on the carrier ground-state localization radius (or impurity size[23]). Hence, we have included the results obtained for a quite different dielectric constant, namely $\epsilon_r = 17.9$, which would correspond to[26] InSb. As may be seen in Fig. 3(a), curves for both dielectric-constant values converge rapidly as the unit-cell size grows. It should be remarked that the mean binding energy decrease as the dielectric constant and the localization radius rise. Figure 3(b) displays how the standard deviation of the binding energy in the FSL also converges rapidly as the unit-cell size increases. As shown in this figure the standard deviation for short-unit cells is quite small, which is in close relation with the fact that the corresponding short-period SL's essentially fulfill the conditions of applicability of an effective-masslike

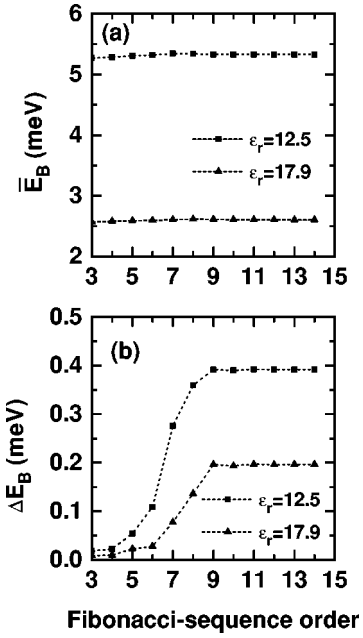

FIG. 3. (a) Mean shallow-donor binding energy $\bar{E}_B$ and (b) the corresponding standard deviation ΔE_B as functions of the Fibonacci-sequence order for different values of the dielectric constant ϵ_r. Squares (triangles) correspond to $\epsilon_r=12.5$ ($\epsilon_r=17.9$), and dashed lines are guides to the eye.

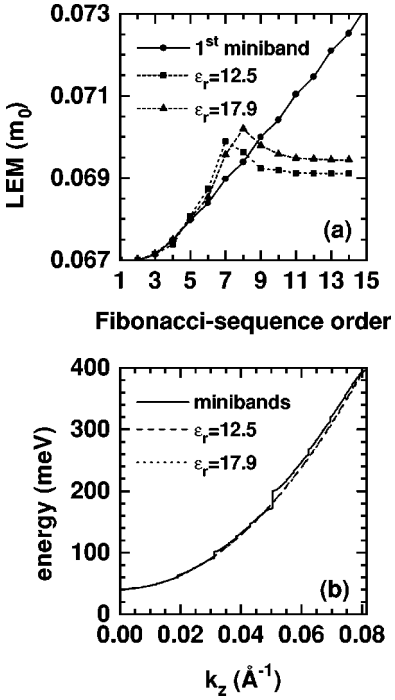

FIG. 4. (a) Mean longitudinal effective mass (LEM) associated to shallow-donor states (in units of the free-electron mass m_0) for a FSL as a function of the Fibonacci-sequence order, together with the FSL first-miniband LEM (circles). Squares (triangles) correspond to $\epsilon_r=12.5$ ($\epsilon_r=17.9$), and lines are guides to the eye. (b) ω_{11}-based FSL conduction-energy band-structure (solid line with vertical steps at the minigaps) and parabolic approximations for the energy, arising from the impurity-associated LEM limits. The dashed (dotted) line stands for $\epsilon_r=12.5$ ($\epsilon_r=17.9$). The layer thicknesses are 11.2 and 16.9 Å for $Ga_{0.8}Al_{0.2}As$ and GaAs, respectively.

theory, which would give a unique value for the impurity associated effective mass for all positions.[23,25]

From the shallow-donor mean binding energies of Fig. 3(a) we may obtain (see Bruno-Alfonso, de Dios-Leyva, and Oliveira[25]) the dependence of the mean LEM on the order of the Fibonacci sequence, as displayed in Fig. 4(a) for two different values of the dielectric constant ϵ_r. We also show the LEM values corresponding to the curvature of the first FSL energy miniband (without impurities), with the FSL electron-energy minibands calculated following a transfer-matrix technique.[12] Notice that the first miniband LEM increases quite rapidly with the Fibonacci order corresponding to the increasingly flat character of the first conduction miniband[23,25] (within the present impurity LEM approach this behavior would correspond to the $\epsilon_r\rightarrow\infty$ limit). Note that the LEM values are plotted for FSL orders 1–14, with the LEM values for orders 1 and 2 being the bulk values for $Ga_{0.8}Al_{0.2}As$ and GaAs, respectively, which are taken as $0.067m_0$. The agreement between all three LEM dependences is apparent in Fig. 4(a) for small-period SL's (orders 3–5). As commented before, this indicates that the first FSL miniband contains the information to describe the corresponding shallow-impurity states within an effective-mass-like theory with a parabolic miniband. For larger periods of the FSL's (orders 6–7) the nonparabolicity of the first miniband enhances the shallow-donor LEM, whereas for FSL's of orders 8–14 the many-miniband effects results in a quasiperiodic limit for the shallow-donor LEM. It should be remarked that the specific behavior of the shallow-donor LEM depends essentially on the relation between the localization radius of the impurity states and the FSL unit-cell length. Therefore, the smaller the dielectric constant (i.e., the smaller the impurity size), the lower Fibonacci order is needed to reach either the enhancement of the donor LEM or the quasiperiodic regime. As the mean-donor LEM dependences for both ϵ_r values appear to converge for order 14 we take these values as the mean LEM's for ideal FSL's of order ∞. As reported by Shung, Sander, and Merlin,[23] the heavier electrons (larger LEM limit) are associated with larger impurity sizes (or ϵ_r values), but here this fact occurs in a subtle way. To clearly show this, we display in Fig. 4(b) the Cantor-like energy band structure for the GaAs-$Ga_{0.8}Al_{0.2}As$ FSL of order 11 (89 elements). Essentially identical curves are obtained for larger Fibonacci orders in these scales of energy and wave number, and the spectrum in the limit of infinite Fibonacci order is the ideal-FSL energy ''band-structure,'' which reflects the asymptotic stability of the FSL energy spectrum as discussed by Maciá, Domínguez-Adame, and Sánchez.[34] The wave number k_z ranges from 0 to π/d_p, where d_p is the fundamental quasiperiod of the FSL, i.e., $d_p=d_a+\tau d_b$, with $\tau=(1+\sqrt{5})/2$ being the golden mean.[28] This wave-number range corresponds[29] to half of the first ''Brillouin minizone'' of the ideal FSL of order ∞. Also shown in Fig. 4(b) are the curves for parabolic energy bands associated to the quasiperiodic limits of the mean LEM for the different ϵ_r values. It is interesting to note that, in the ranges of energy and wave number shown, both parabolic curves essentially coincide (as a consequence of the small difference between the corresponding LEM values) and reproduce the overall behavior of the FSL band structure.

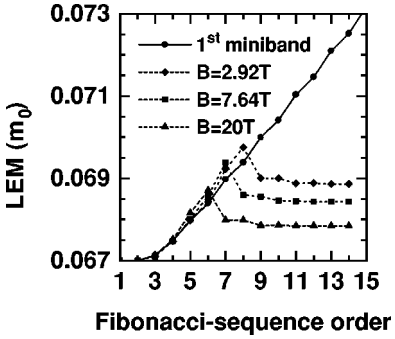

FIG. 5. Mean-longitudinal effective mass (LEM; in units of the free-electron mass m_0) associated with the energy of the conduction-electron ground-state Landau level for in-plane magnetic fields as a function of the Fibonacci-sequence order, together with the FSL first-miniband LEM (circles). Diamonds, squares, and triangles correspond to magnetic field values of 2.92, 7.64, and 20 T, respectively (field intensities are scaled by τ^2). Lines are guides to the eye.

The same general conclusions arise in the study of the conduction-electron Landau levels in the FSL under in-plane magnetic fields. Figure 5 shows the dependence on the Fibonacci order of the mean LEM for three magnetic-field intensities scaled[28,32] by τ^2. The magnetic field imposes a length scale characterized by the Landau radius $l_B=\sqrt{\hbar/eB}$, which increases when the field intensity is lowered. As discussed above for the LEM associated to shallow-donor states in GaAs-(Ga,Al)As FSL's heavier electrons in the ideal FSL are associated to larger localization radii. It is worth noticing that the length scales studied in Fig. 5 are quite different, whereas the corresponding LEM limit values are very similar: for thin barrier FSL's, one obtains that the limiting LEM varies less than 2% for quite different strengths of the confining potential (Coulomb or magnetic), i.e., localization lengths. Therefore, all the corresponding LEM values may be associated with the curvature of the E vs k_z parabolas, which essentially reproduce the Cantor-like structure of the extended scheme of the FSL energy spectrum [as may be seen in Fig. 4(b)]. In that sense, therefore, for thin barriers FSL's, the mean LEM limit weakly depends on the nature of the conduction-electron (or impurity) state and localization length, and is closely related to the fractal-like ''band structure.'' On the other hand, it should be noticed in Figs. 4(a) and 5 that, for FSL's in the nonparabolic one-miniband regime (orders 6–7), as expected heavier electrons are associated to shorter localization radii in contrast with the result obtained here for the quasiperiodic limit of large FSL cells.

All results discussed above correspond to FSL's with barrier and well thicknesses of $d_a=11.2$ Å and $d_b=16.9$ Å, respectively, which have two special properties: weak barriers and $d_b/d_a\simeq\tau$ (self-similarity condition). Now, for comparison with the results in Fig. 4, we display in Fig. 6 the LEM associated with shallow-impurity states in a FSL with $d_a=d_b=33.9$ Å. The above discussion for Fig. 4(a) also applies for Fig. 6(a), except for the relative difference between the LEM limit values, which is much larger. This fact is apparent in Fig. 6(b), where the parabolic bands corresponding to those LEM limiting values separate and do not reproduce the band structure so well, in contrast with the results in

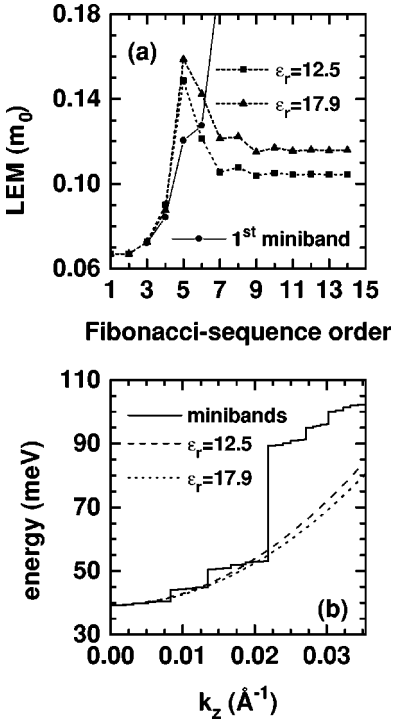

FIG. 6. As in Fig. 4, but here both the barrier and well thicknesses are 33.9 Å.

Fig. 4(b). As a matter of fact, the band structure of this FSL is so singular that no parabola would properly follow its overall behavior, but rather only its shape for small wave numbers. So, the singular geometry of the FSL energy band structure implies a larger dependence of the shallow-donor LEM on the localization length of the associated impurity states. In this respect, Fig. 7 displays the energy band structure for different GaAs-$Ga_{0.8}Al_{0.2}$As FSL's in the first Brillouin minizones.[29] As may be noticed, the energy-band structures for thin-barrier FSL's (1–3) may be clearly approximated by parabolic LEM-energy curves, whereas for thick-barrier FSL's (4–5) the whole concept of a LEM begins to break down.

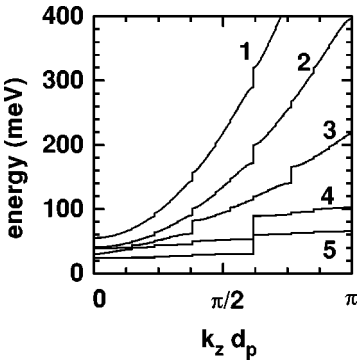

FIG. 7. Conduction minibands of FSL's generated by the sequence ω_{11} (89 elements in the unit cell) for different values of the layer thicknesses. The Bloch wave number is k_z and d_p is the fundamental quasiperiod of the FSL. The barrier widths for curves labeled 1–3 (4–5) is 11.2 Å (33.9 Å), and the well thicknesses are 11.2, 16.9, 33.9, 33.9, and 51.2 Å, for curves 1–5, respectively. Vertical lines are guides to the eye at the minigaps.

IV. CONCLUSIONS

We have calculated the energy of the shallow-impurity ground states as well as the energy of the ground conduction Landau level (under in-plane magnetic fields), in GaAs-(Ga,Al)As FSL's. These SL's consists of periodic stackings of Fibonacci-sequenced unit cells, and we analyzed the quasiperiodic limit of large unit-cell sizes, and the relation between the mean LEM and the localization length of the corresponding electronic or impurity states. For the mean energy of the impurity or magnetic states one associates a mean LEM, which weakly depends on the localization radius of the corresponding wave functions. Heavier localized electrons are associated with larger localization lengths. The mean LEM experiences small changes for large variations of the localization radius in the case of thin-barrier SL's, and its values are associated with parabolic envelopes of the FSL energy-band structure. As the barriers become thicker this regime breaks down and the singular geometry of the FSL energy-band structure leads to an increasing dependence of the shallow-impurity LEM on the localization length of the corresponding impurity states.

One should stress that the approach used in the present calculation is not restrictive to Fibonacci-like SL's and similar theoretical studies may be performed for other kinds of semiconductor heterostructures (periodic or aperiodic) of interest such as Thue-Morse or random SL's. Finally, as pointed out by Shung, Sander, and Merlin,[23] the experimental observation of the effects of quasiperiodicity on the (electron or shallow impurity) longitudinal-effective mass could be performed by far-infrared cyclotron-resonance measurements with in-plane magnetic fields (or far-infrared spectroscopic measurements on conduction-to-donor states transitions) on such SL's so that electrons in a Landau (or impurity) level tunnel through many SL layers.

ACKNOWLEDGMENTS

This work was partially supported by Brazilian agencies FAPERJ, FAPESP, FAEP-UNICAMP, and CNPq.

*Electronic address:alexys@if.uff.br

[1] D. Shechtman, I. Blech, D. Gratias, and J. W. Cahn, Phys. Rev. Lett. **53**, 1951 (1984).
[2] J. P. Lu and J. L. Birman, Phys. Rev. B **36**, 4471 (1987).
[3] T. Ninomiya, J. Non-Cryst. Solids **117**, 777 (1990); T. Matsuda, Y. Sakabe, I. Ohara, and U. Mizutani, *ibid.* **117**, 804 (1990); T. Fujiwara, *ibid.* **117**, 844 (1990).
[4] T. Janssen, Ferroelectrics **104**, 51 (1990).
[5] A. Inaba, S. Ishida, T. Matsuo, K. Shibata, and P. Tsai, Philos. Mag. Lett. **74**, 381 (1996).
[6] G. Dell'Acqua, M. Krajčí, and J. Hafner, J. Phys.: Condens. Matter **9**, 10 725 (1997).
[7] D. Levine and P. J. Steinhardt, Phys. Rev. Lett. **53**, 2477 (1984).
[8] S. Ostlund, R. Pandit, D. Rand, H. J. Schellnhuber, and E. D. Siggia, Phys. Rev. Lett. **50**, 1873 (1983).
[9] C. de Lange and T. Janssen, Phys. Rev. B **28**, 195 (1983).
[10] M. Kohmoto, L. P. Kadanoff, and C. Tang, Phys. Rev. Lett. **50**, 1870 (1983); M. Kohmoto and Y. Oono, Phys. Lett. **102A**, 145 (1984); M. Kohmoto, B. Sutherland, and C. Tang, Phys. Rev. B **35**, 1020 (1987).
[11] R. Merlin, K. Bajema, R. Clarke, F.-Y. Juang, and P. K. Bhattacharya, Phys. Rev. Lett. **55**, 1768 (1985).
[12] F. Laruelle and B. Etienne, Phys. Rev. B **37**, 4816 (1988).
[13] A. A. Yamaguchi, T. Saiki, T. Tada, T. Ninomiya, T. Kobayashi, M. Kuwata-Gonokami, and T. Yao, Solid State Commun. **75**, 955 (1990).
[14] D. Munzar, L. Bočáek, J. Humlíček, and K. Ploog, J. Phys.: Condens. Matter **6**, 4107 (1994).
[15] M. Dinu, M. R. Melloch, and D. D. Nolte, J. Appl. Phys. **79**, 3787 (1996).
[16] E. Diez, F. Domínguez-Adame, E. Maciá, and A. Sánchez, Phys. Rev. B **54**, 16 792 (1996).
[17] E. Maciá and F. Domínguez-Adame, Phys. Rev. Lett. **76**, 2957 (1996).
[18] J. Arriaga and V. R. Velasco, J. Phys.: Condens. Matter **9**, 8031 (1997).
[19] F. Laruelle, B. Etienne, J. Barrau, K. Khirouni, J. C. Brabant, T. Amand, and M. Brousseau, Surf. Sci. **228**, 92 (1990).
[20] M. Castro and F. Domínguez-Adame, Phys. Lett. A **225**, 321 (1997).
[21] P. Carpena, Phys. Lett. A **231**, 439 (1997).
[22] E. Reyes-Gómez , C. A. Perdomo-Leiva, L. E. Oliveira, and M. de Dios-Leyva, J. Phys.: Condens. Matter **10**, 3557 (1998).
[23] K. W.-K. Shung, L. M. Sander, and R. Merlin, Phys. Rev. Lett. **61**, 455 (1988).
[24] R. Merlin, IEEE J. Quantum Electron. **24**, 1791 (1988).
[25] A. Bruno-Alfonso, M. de Dios-Leyva, and L. E. Oliveira, Phys. Rev. B **57**, 6573 (1998).
[26] C. Kittel, *Introduction to Solid State Physics*, 7th ed. (Wiley, New York, 1996).
[27] F. J. Ribeiro, A. Bruno-Alfonso, and A. Latgé, Phys. Rev. B **57**, 13 010 (1998).
[28] Y. Y. Wang and J. C. Maan, Phys. Rev. B **40**, 1955 (1989).
[29] D. Toet, Dissertation, Universitaät Konstanz, Facultät für Physik, 1992.
[30] A. Bruno-Alfonso, E. Reyes-Gómez, L. E. Oliveira, and M. de Dios-Leyva, J. Appl. Phys. **78**, 1379 (1995); Appl. Phys. Lett. **67**, 536 (1995).
[31] J. B. Xia and W. J. Fan, Phys. Rev. B **40**, 8508 (1989).
[32] M. de Dios-Leyva, A. Bruno-Alfonso, E. Reyes-Gómez, and L. E. Oliveira, J. Phys.: Condens. Matter **7**, 9799 (1995); M. de Dios-Leyva, A. Bruno-Alfonso, and L. E. Oliveira, *ibid.* **9**, 1005 (1997).
[33] G. Bastard, Phys. Rev. B **24**, 4714 (1981).
[34] E. Maciá, F. Domínguez-Adame, and A. Sánchez, Phys. Rev. B **49**, 9503 (1994).